ISSN 1070-3284, Russian Journal of Coordination Chemistry, 2019, Vol. 45, No. 10, pp. 675–679. © Pleiades Publishing, Ltd., 2019.
Russian Text © The Author(s), 2019, published in Koordinatsionnaya Khimiya, 2019, Vol. 45, No. 10, pp. 579–583.

Magnetic Properties of the Dicationic Iron *o*-Quinone Complexes with the Pyridinophane Ligands: A Quantum Chemical Study

A. G. Starikov[a], M. G. Chegerev[a], A. A. Starikova[a, *], and V. I. Minkin[a]

[a] *Institute of Physical and Organic Chemistry, Southern Federal University, Rostov-on-Don, Russia*

**e-mail: alstar@ipoc.sfedu.ru*

Received March 28, 2019; revised April 4, 2019; accepted April 10, 2019

Abstract—Computer modeling of the dicationic iron *o*-benzoquinone complexes with the 2,11-diaza[3.3]-(2,6)pyridinophane ligands is performed. The ground states of the studied compounds are the low-spin isomers. Strong antiferromagnetic exchange interactions are predicted to take place between lone electrons of the trivalent iron ion and the radical-anionic form of the redox-active ligand. The compound capable of undergoing crossover is revealed by the variation of substituents in the tetraazamacrocyclic base.

Keywords: iron complexes, tetraazamacrocyclic ligands, *o*-benzoquinone, spin-crossover, magnetic properties, quantum chemical calculations, density functional theory

DOI: 10.1134/S1070328419090082

INTRODUCTION

Coordination compounds of transition metals with radical ligands evoke increased interest of specialists in the area of coordination and organometallic chemistry due to their unusual magnetic behavior [1, 2]. A reasonable design of these structures provides wide challenges for the development of dynamic materials, devices of information storage, recording units, and quantum computers [3, 4]. The *o*-benzoquinone derivatives with redox-active properties represent an abundant type of radical ligands [5]. Transition metal complexes with these organic molecules can demonstrate rearrangements via the mechanism of spin-crossover (SCO) [4] or valence tautomerism [6–8] accompanied by switching spin states.

There are several methods for the construction of magnetically active coordination compounds with *o*-quinones. The first one includes two redox ligands and mono- or bidentate bases with donor nitrogen atoms building the coordination sphere of the metal to an octahedron [9]. These complexes are classical systems of valence tautomerism. Another structural motif has recently been proposed: the electroneutral adduct of the transition metal bis(chelate) with one *o*-benzoquinone ligand in which thermally initiated spin rearrangements occur [10, 11]. The cationic complexes containing one redox-active ligand and tetradentate macrocyclic nitrogen-containing base represent the third type of compounds demonstrating magnetic bistability [12–14]. Constructed in this way molecules can manifest both valence tautomerism [12] and SCO [13, 14] depending on the nature of the tetraazamacrocycle and metal.

The dicationic iron di-*tert*-butyl-*o*-benzoquinone complex with *N*,*N*'-dimethyl-2,11-diaza[3.3]-(2,6)pyridinophane, being the first example of compounds containing the low-spin (LS) ferric iron and semiquinone (SQ) form of the redox-active ligand, has recently been synthesized [15]. The authors [15] were interested in the study of the oxidation, catalytic activity, and ability of this system to imitate dioxygenase. This compound is a structural analog of the monocationic iron complex with *N*,*N*'-di-*tert*-butyl-2,11-diaza[3.3]-(2,6)py-ridinophane exhibiting SCO [14].

In this work, we used quantum chemical methods to study the geometric, energetic, and magnetic characteristics of iron *o*-benzoquinone complexes **I** (R_1 = CH_3; R_2 = H), **II** (R_1 = CH_3; R_2 = Cl), and **III** (R_1 = *tert*-Bu; R_2 = H) with the pyridinophane derivatives. The task of the study was to reveal the influence of substituents in the redox-active and tetraazamacrocyclic ligands on the possibility of the thermally initiated spin transition to occur.

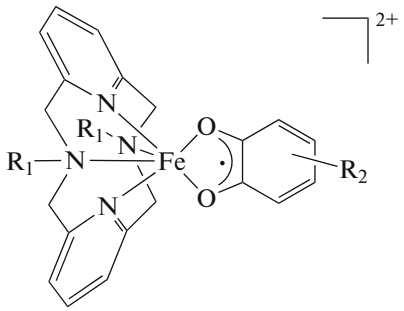

I–III (R_1 = CH_3, *tert*-Bu; R_2 = H, Cl)

Table 1. Spin (S), total energy (E), squared spin operator (S^2), and spin density on the iron ion $\left(q_s^M\right)$ and redox-active ligand $\left(q_s^L\right)$ in the isomers of dicationic complexes **I–III** (R_1 = CH_3, *tert*-Bu; R_2 = H, Cl) calculated by the DFT UTPSSh/6-311++G(d,p) method

Isomer	S	E, au	S^2	q_s^M	q_s^L
I ($R_1 = CH_3$; $R_2 = H$)					
$_{LS}Fe^{III}SQ$	2/2	–2485.93717	2.042	1.13	1.02
BS	0	–2485.94721	0.667	0.72	–0.74
$_{HS}Fe^{III}SQ$	6/2	–2485.91384	12.014	4.23	1.38
BS	4/2	–2485.92421	6.662	4.04	–0.47
II ($R_1 = CH_3$; $R_2 = Cl$)					
$_{LS}Fe^{III}SQ$	2/2	–4324.40185	2.043	1.07	1.05
BS	0	–4324.41189	0.691	0.74	–0.75
$_{HS}Fe^{III}SQ$	6/2	–4324.38017	12.015	4.14	1.40
BS	4/2	–4324.38940	6.679	4.03	–0.47
III (R_1 = *tert*-Bu; R_2 = H)					
$_{LS}Fe^{III}SQ$	2/2	–2721.88466	2.062	1.11	1.06
BS	0	–2721.89029	0.752	0.78	–0.79
$_{HS}Fe^{III}SQ$	6/2	–2721.86755	12.014	4.03	1.49
BS	4/2	–2721.87801	6.649	3.84	–0.43

CALCULATION PROCEDURE

The calculations were performed using the Gaussian 09 program [16] by the density functional theory (DFT) with the UTPSSh functional [17, 18] and extended 6-311++G(d,p) basis set, the combination of which correctly reproduced the energetic characteristics of SCO in the cationic complexes [19–25]. Stationary points were localized on the potential energy surface (PES) by the full geometry optimization of the molecular structures with checking the DFT stability of the wave function. The exchange interaction parameters (J, cm^{-1}) were calculated in the framework of the broken symmetry (BS) formalism [26] using the earlier proposed equation [27]. The graphical images of the molecular structures were obtained using the ChemCraft program [28].

RESULTS AND DISCUSSION

According to the calculations, the ground state of compound **I** (R_1 = CH_3; R_2 = H) is the LS isomer $_{LS}Fe^{III}SQ$ on the doublet PES including the trivalent metal ion and the SQ form of the redox-active ligand (Fig. 1, Table 1). The calculated bond lengths in the coordination site and benzoquinone ring correlate well with the values determined by X-ray diffraction analysis [15]. Strong exchange interactions of the antiferromagnetic character ($J = -1603$ cm^{-1}, see Table 2) were predicted to take place in the discussed electronic isomer (electromer [29]), which is also consistent with the experimental data indicating diamagnetism of the complex [15]. A considerable overlapping of the orbitals of the iron and oxygen atoms (Fig. 2) leads to a decrease in the amount of the spin density on the metal and redox-active ligand in the BS state (Table 1).

The $_{HS}Fe^{III}SQ$ isomer containing the high-spin (HS) trivalent iron ion and semiquinone was localized on the sextet PES. As follows from the data presented in Table 1, the amount of the spin density on the metal atom is 4.23, which is lower than the value expected for five lone electrons. At the same time, this parameter for the redox-active ligand is equal to 1.38 (Table 1). Therefore, the electron density is transferred from the metal ion to the donor atoms of *o*-benzoquinone and *N*,*N*'-dimethyl-2,11-diaza[3.3]-(2,6)pyridinophane (Fig. 1) in the HS isomer $_{HS}Fe^{III}SQ$. The calculation of the BS state followed by the analysis of exchange interactions indicates a strong antiferromagnetic coupling leading, as in the LS isomer $_{LS}Fe^{III}SQ$, to a decrease in q_s^M and q_s^L (Table 1). The calculated difference in energies between the electromers of complex **I** (R_1 = CH_3; R_2 = H) exceeds the values characteristic for SCO in the iron complexes [1] and does not allow one to expect that the thermally initiated spin transition would occur in complex **I** (Table 2).

It is known [13] that the introduction of electron-withdrawing substituents into the redox-active fragment facilitates the thermally induced SCO in the iron

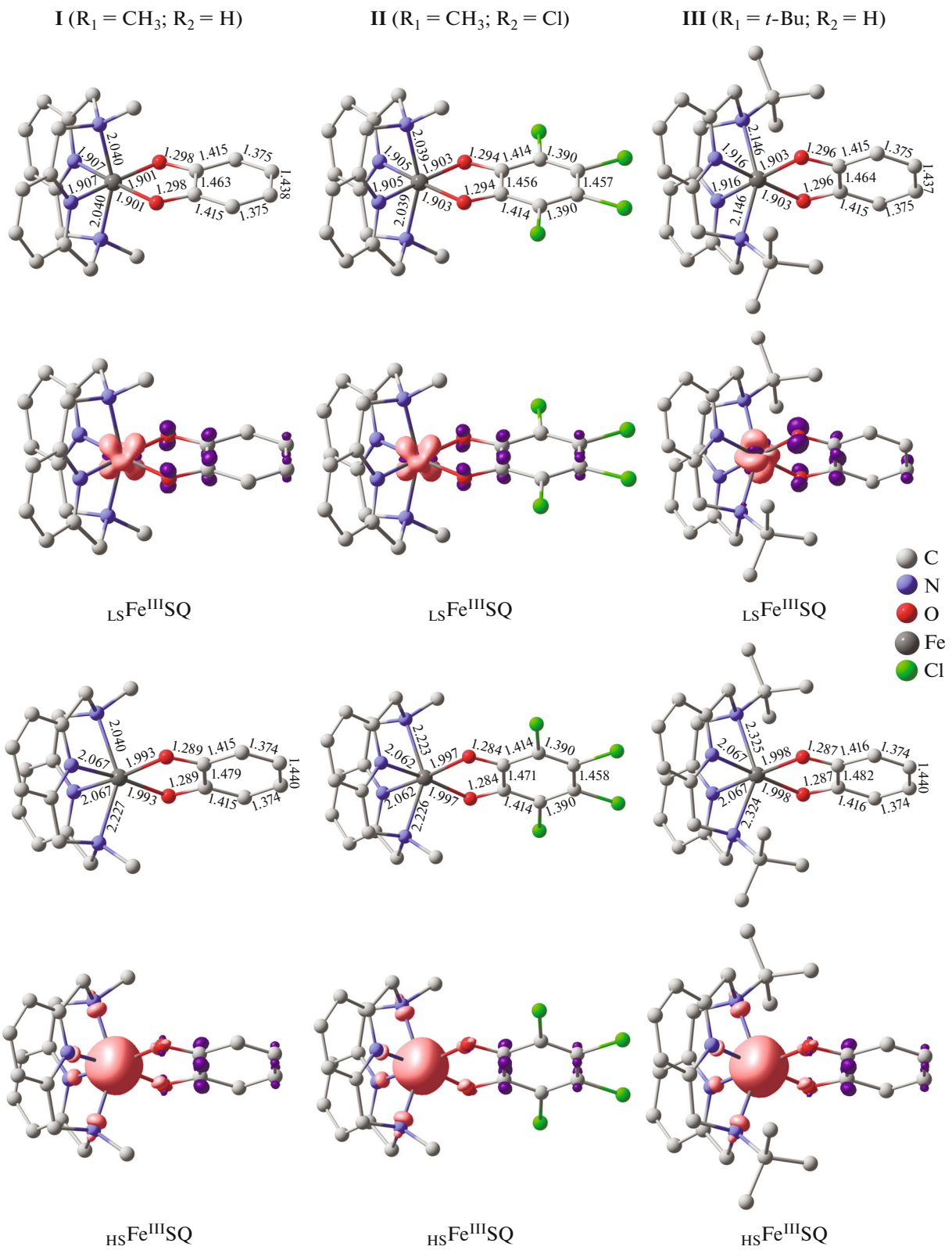

Fig. 1. Geometric characteristics and spin density distribution in the isomers of dicationic complexes **I–III** (R_1 = CH_3, *tert*-Bu; R_2 = H, Cl) calculated by the DFT UTPSSh/6-311++G(d,p) method. Hydrogen atoms are omitted for clarity, bond lengths are given in Å, all structures have the charge +2, and cutoff = 0.02.

Table 2. Spin (S), relative energy taking into account exchange interactions (ΔE), and exchange interaction parameter (J) in the isomers of dicationic complexes **I–III** (R_1 = CH_3, *tert*-Bu; R_2 = H, Cl) calculated by the DFT UTPSSh/6-311++G(d,p) method

Isomer	S	ΔE*, kcal/mol	J, cm^{-1}
I ($R_1 = CH_3$; R_2 = H)			
$_{LS}Fe^{III}SQ$	2/2	0.0	−1603
$_{HS}Fe^{III}SQ$	6/2	14.4	−425
II ($R_1 = CH_3$; R_2 = Cl)			
$_{LS}Fe^{III}SQ$	2/2	0.0	−1630
$_{HS}Fe^{III}SQ$	6/2	14.1	−380
III (R_1 = *tert*-Bu; R_2 = H)			
$_{LS}Fe^{III}SQ$	2/2	0.0	−943
$_{HS}Fe^{III}SQ$	6/2	7.7	−428

* ΔE were calculated relative to the LS isomer of the complex.

o-semiquinone complexes with the tetraazamacrocyclic ligands. Derivative **II** (R_1 = CH_3; R_2 = Cl) was studied to search for a compound capable of undergoing spin transitions on the Fe^{3+} ion. The calculations showed that the chlorine substituents in the radical ligand exerted no substantial effect on the energetic and magnetic characteristics of the electromers of this complex (Tables 1, 2; Fig. 1). The destabilization of the $_{HS}Fe^{III}SQ$ isomer with respect to the $_{LS}Fe^{III}SQ$ LS structure by 14.1 kcal/mol indicates that the HS state is thermally unattainable. Strong antiferromagnetic exchange interactions (J = −1630 cm^{-1}) leading to diamagnetism of complex **II** (R_1 = CH_3; R_2 = Cl) in a wide temperature range are expected to occur in the electromer on the doublet PES.

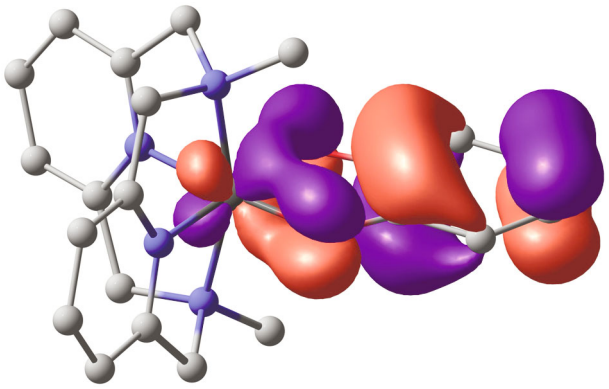

Fig. 2. Shape of the magnetic orbital of the $_{LS}Fe^{III}SQ$ isomer of complex **I** (R_1 = CH_3; R_2 = H) according to the DFT UTPSSh/6-311++G(d,p) calculations. Hydrogen atoms are omitted for clarity, and cutoff = 0.036.

The ability of bulky substituents at the donor atoms of the tetraazamacrocyclic ligands to impede the formation of the LS isomer characterized by shorter coordination bonds has earlier been shown experimentally [14] and theoretically [21, 22]. This effect reduces the difference in energies between the electromers to the values favoring the occurrence of the thermally controlled SCO. Taking into account the aforesaid, we studied complex **III** (R_1 = *tert*-Bu; R_2 = H). The calculations showed that the replacement of the methyl substituents at the nitrogen atoms of the pyridinophane ligand by *tert*-butyl groups was accompanied by changes in the geometric and energetic characteristics of the electromers (Tables 1, 2; Fig. 1). For example, the Fe–N distance is elongated by 0.1 Å compared to the values calculated for the isomers of complex **I** (R_1 = CH_3; R_2 = H). This results in a decrease in the stability of the LS structure and narrowing of the energy gap between the electromers $_{LS}Fe^{III}SQ$ and $_{HS}Fe^{III}SQ$ to 7.7 kcal/mol, thus providing a possibility of the spin transition to occur on the iron ion. The exchange interactions in compound **III** (R_1 = *tert*-Bu; R_2 = H), as those in the systems considered above, are strongly antiferromagnetic. Therefore, the expected rearrangement $_{LS}Fe^{III}SQ \rightleftarrows {}_{HS}Fe^{III}SQ$ will be accompanied by the transition of the complex from the diamagnetic (S = 0) to paramagnetic quintet (S = 4/2) state, which enables us to consider complex **III** (R_1 = *tert*-Bu; R_2 = H) as a candidate for the design of molecular switches.

Thus, it was established by the quantum chemical modeling of the dicationic iron *o*-semiquinone complexes with the pyridinophane derivatives that the electron-withdrawing groups in the radical ligand exerted no appreciable effect on the properties of the studied coordination compounds, whereas the variation of the substituents at the nitrogen atoms of the tetradentate base was accompanied by a change in the geometric and energetic characteristics of the isomers. The strong antiferromagnetic exchange interactions leading to diamagnetism of the ground state were predicted to occur between spins of lone electrons of the trivalent iron ion and radical-anionic form of *o*-quinone. The dicationic iron *o*-benzoquinone complex with *N*,*N*'-di-*tert*-butyl-2,11-diaza[3.3]-(2,6)pyridinophane capable of exhibiting thermally initiated SCO was proposed. The earlier synthesis of coordination compound **I** (R_1 = CH_3; R_2 = H) [15] allows one to expect the preparation of its analog containing *tert*-butyl groups at the donor nitrogen atoms.

FUNDING

This work was supported by the Ministry of Science and Higher Education of the Russian Federation (state task no. 4.1774.2017/4.6).

CONFLICT OF INTEREST

The authors declare that they have no conflicts of interest.

REFERENCES

1. *Stable Radicals: Fundamentals and Applied Aspects of Odd-Electron Compounds*, Hicks R.G., Ed., Chichester: Wiley, 2010.
2. Demir, S., Jeon, I.-R., Long, J.R., and Harris, T.D., *Coord. Chem. Rev.*, 2015, vols. 289–290, p. 149.
3. Sato, O., *Nature Chem.*, 2016, vol. 8, no. 7, p. 644.
4. *Spin-Crossover Materials: Properties and Applications*, Halcrow M.A., Ed., Chichester: Wiley, 2013.
5. Shultz, D.A., in *Magnetism: Molecules to Materials II*, Miller, J.S. and Drillon, M., Eds., New York: Wiley, 2001, p. 281.
6. Tezgerevska, T., Alley, K.G., and Boskovic, C., *Coord. Chem. Rev.*, 2014, vol. 268, p. 23.
7. Zolotukhin, A.A., Bubnov, M.P., Cherkasov, V.K., et al., *Russ. J. Coord. Chem.*, 2018, vol. 44, no. 4, p. 272. https://doi.org/10.1134/S1070328418040085
8. Protasenko, N.A., Poddel'sky, A.I., Bogomyakov, A.S., et al., *Inorg. Chim. Acta*, 2019, vol. 489, p. 1.
9. Buchanan, R.M. and Pierpont, C.G., *J. Am. Chem. Soc.*, 1980, vol. 102, p. 4951.
10. Starikova, A.A. and Minkin, V.I., *Russ. Chem. Rev.*, 2018, vol. 87, no. 11, p. 1049.
11. Ivakhnenko, E.P., Koshchienko, Y.V., Knyazev, P.A., et al., *Russ. J. Coord. Chem.*, 2016, vol. 42, no. 4, p. 252. https://doi.org/10.1134/S1070328416040011
12. Bencinia, A., Caneschia, A., Carbonera, C., et al., *J. Mol. Struct.*, 2003, vol. 656, nos. 1–3, p. 141.
13. Floquet, S., Simaan, A.J., Rivière, E., et al., *Dalton Trans.*, 2005, no. 9, p. 1734.
14. Graf, M., Wolmershauser, G., Kelm, H., et al., *Angew. Chem., Int. Ed. Engl.*, 2010, vol. 49, no. 5, p. 950.
15. Koch, W.O., Schünemann, V., Gerdan, M., et al., *Chem.-Eur. J.*, 1998, vol. 4, no. 7, p. 1255.
16. Frisch, M.J., Trucks, G.W., Schlegel, H.B., et al., *Gaussian-09. Revision E. 01*, Wallingford: Gaussian, 2013.
17. Tao, J.M., Perdew, J.P., Staroverov, V.N., and Scuseria, G.E., *Phys. Rev. Lett.*, 2003, vol. 91, no. 14, p. 146401.
18. Staroverov, V.N., Scuseria, G.E., Tao, J., and Perdew, J.P., *J. Chem. Phys.*, 2003, vol. 119, no. 23, p. 12129.
19. Bannwarth, A., Schmidt, S.O., Peters, G., et al., *Eur. J. Inorg. Chem.*, 2012, no. 16, p. 2776.
20. Cirera, J. and Paesani, F., *Inorg. Chem.*, 2012, vol. 51, no. 15, p. 8194.
21. Starikov, A.G., Starikova, A.A., and Minkin, V.I., *Dokl. Chem.*, 2016, vol. 467, no. 1, p. 83.
22. Starikova, A.A., Chegerev, M.G., Starikov, A.G., and Minkin, V.I., *Comp. Theor. Chem.*, 2018, vol. 1124, p. 15.
23. Starikova, A.A. and Minkin, V.I., *Russ. J. Coord. Chem.*, 2018, vol. 44, no. 8, p. 483. https://doi.org/10.1134/S1070328418080079
24. Starikov, A.G., Starikova, A.A., Chegerev, M.G., and Minkin, V.I., *Russ. J. Coord. Chem.*, 2019, vol. 45, no. 2, p. 105. https://doi.org/10.1134/S1070328419020088
25. Starikova, A.A., Metelitsa, E.A., and Minkin, V.I., *Russ. J. Coord. Chem.*, 2019, vol. 45, no. 6, p. 411. https://doi.org/10.1134/S1070328419060095
26. Noodleman, L., *J. Chem. Phys.*, 1981, vol. 74, no. 10, p. 5737.
27. Shoji, M., Koizumi, K., Kitagawa, Y., et al., *Chem. Phys. Lett.*, 2006, vol. 432, nos. 1–3, p. 343.
28. Chemcraft. Version 1.7. 2013. http://www.chemcraftprog.com
29. Bally, T., *Nature Chem.*, 2010, vol. 2, no. 3, p. 165.

Translated by E. Yablonskaya